Accelerating EB's Potential: Understanding the Effects of Dose Rate in Electron-beam Polymerization

Sage M. Schissel,[1] Stephen C. Lapin,[2] and Julie L. P. Jessop[1]
[1]Department of Chemical & Biochemical Engineering, University of Iowa, Iowa City, IA
[2]PCT Engineered Systems, LLC, Davenport, IA

Abstract:

Properties of some materials synthesized via electron-beam (EB) polymerization appear dependent upon the rate at which the initiating dose is delivered (i.e., dose rate effects). The relationship among dose rate, glass transition temperature and conversion was explored for an acrylic monomer series. A preliminary predictive relationship was developed to estimate the magnitude of the dose rate effect, enabling scale-up of process variables for polymers prone to dose rate effects.

Introduction:

Electron-beam (EB) polymerization is used extensively to produce millions of tons of film, coating, ink, and adhesive products each year.[1] EB curing is a rapid, sustainable process, requiring no environmentally damaging solvents and less energy than other polymerization methods.[2-4] Furthermore, in contrast to photopolymerization, EB polymerization is not hindered by fillers or pigments, allowing for widespread property tuning through the use of additives.

In spite of the established commercial use of EB-curing technology, published research describing the fundamental aspects of EB polymerization is limited.[2,3,5-7] Large gaps exist in the understanding of EB kinetics and how EB-cured polymer properties are influenced by processing variables. One area where this knowledge gap is especially problematic is the application of dose rate and how dose rate affects polymer properties.

While the dose (*i.e.*, the energy imparted to the sample) can be held constant by adjusting the beam current and line speed (see Equation 1), the speed at which the dose is delivered – dose rate – changes.

$$Dose = \frac{Beam\ Current * K}{Line\ Speed} \quad (1)$$

Altering the dose rate can cause property changes in the cured polymer, known as dose rate effects.

Avoiding dose rate effects, particularly in commercial applications, may be difficult. Many new formulations are tested on a slower pilot line or lab equipment, where the materials and required dose levels are optimized. Then, the beam current and line speed are scaled for commercial production requirements. If dose rate effects and their magnitude were consistent, adjustments could be made during this scale-up process; however, some formulations are more prone to dose rate effects than others, suggesting formulation chemistry has an impact on the magnitude of the dose rate effects.

In this study, a series of acrylate monomers was investigated, and a strong correlation was observed between monomer chemical structure and the magnitude of the dose rate effect found in two, commonly reported polymer properties: conversion and glass transition temperature. From these data, a rudimentary structure/processing conditions/properties relationship was established, enabling predictions of a formulation's dose rate effect by comparing its response to different doses. This foundational research will allow more thorough investigations into the cause of dose rate effects in EB-cured polymers, providing a more reliable means of scaling to production modes.

Experimental:

Materials

A series of five monomers was chosen to investigate the impact of monomer chemistry on the magnitude of the dose rate effect: phenyl acrylate (PA, MP Biomedicals), benzyl acrylate (BA, MP Biomedicals), 2-phenylethyl acrylate (PEA, Polysciences), 2-phenoxyethyl acrylate (POEA, TCI America), and 2-hydroxy-3-phenoxypropyl acrylate (HPOPA, Sartomer) (Fig 1).

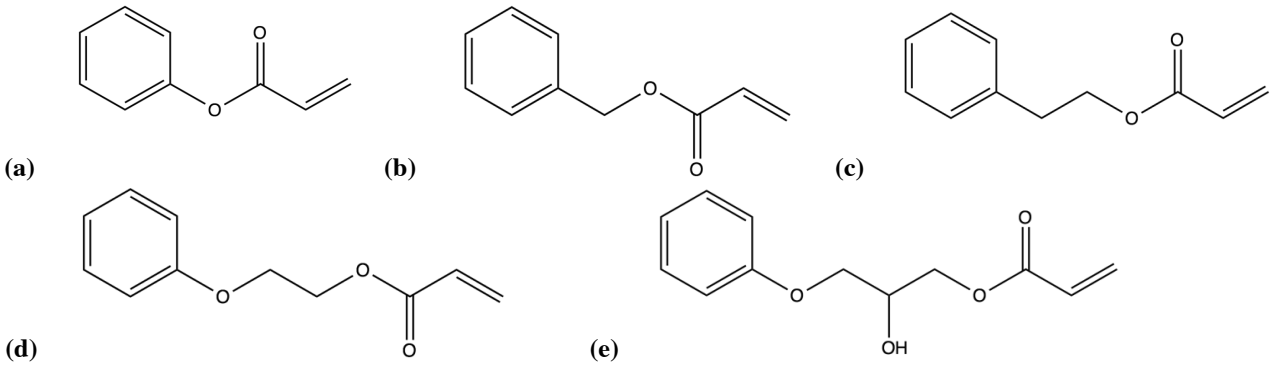

Figure 1. The chemical structures of the 5-monomer series: (a) PA, (b) BA, (c) PEA, (d) POEA, and (e) HPOPA.

To enable Raman conversion measurements, each monomer contains a phenyl group and an acrylate moiety.[8] The number of chemical bonds separating the phenyl ring from the acrylate moiety differentiates the monomers and is incrementally increased across the series. An aliphatic urethane diacrylate oligomer, Ebecryl 8807 (proprietary structure, Allnex), was added to each monomer to improve the film properties of the samples and allowed for mechanical-property testing. All materials were used as received and stored at room temperature.

Methods

EB Film Preparation

Each formulation consisted of a 50/50, by weight, mixture of monomer and oligomer. Because of the high viscosity of the oligomer, the formulations were heated to approximately 60°C to allow mixing of the monomer and oligomer. Once heated, formulations were stirred using a drill with a paddle mixer attachment.

Samples for EB curing were prepared by first treating 4 x 3.25 inch glass slides using two coats of Rain-X® 2-in-1 glass cleaner and rain repellent. Next, two layers of lab tape (total thickness ~180 μm) were placed on either side of the glass to be used as spacers. A large droplet, approximately 1 mL, of a formulation was then placed near the top of the slide, between the pieces of tape, and covered with a piece of silicone-coated, 34-μm thick polyethylene terephthalate (PET). A straight edge was drawn across the PET to form a uniform film underneath.

The samples on the glass slides were polymerized by EB irradiation through the PET film using an EB accelerator equipped with a variable-speed, fiberglass carrier web (BroadBeam EP Series, PCT Engineered Systems, Inc.). Three different doses (15, 30, and 60 kGy) and three different line speeds (20, 100, and 200 ft/min) were used to cure the films. Accelerating voltage and N_2 flow rate were held constant at 250 kV and 17 SCFM, respectively. Once polymerized, the films were removed from the glass slides and cut into rectangles measuring 6.25 x 25 mm for characterization. The use of silanized (Rain-X®-treated) glass and silicone-coated PET assisted in the release of the polymer film.

Raman Spectroscopy

Raman spectroscopy was used to determine conversion of the polymer films. In order to eliminate error from instrumental variations, a reference peak was used. Previous work has established the reaction peak at 1636 cm^{-1} (indicative of the –C=C– bond in the acrylate moiety) and the reference peak at 1613 cm^{-1} (indicative of the –C=C– bonds in the phenyl ring) (Fig 2).[8]

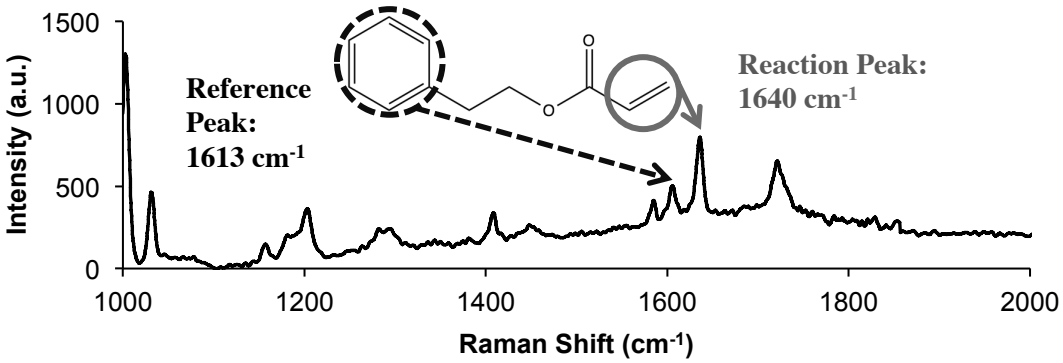

Figure 2. Raman spectrum of PEA, identifying the correlation between chemical structure and peak location. The reference peak at 1613 cm^{-1} represents the –C=C– in the phenyl ring, and the reaction peak at 1640 cm^{-1} represents the –C=C– in the acrylate moiety.

Conversion, α, was calculated using the following equation:

$$\alpha = 1 - \frac{I_{rxn}(P)/I_{ref}(P)}{I_{rxn}(M)/I_{ref}\,(M)} \qquad (2)$$

where $I_{rxn}(P)$ and $I_{ref}(P)$ are the peak intensities of the reaction and reference peak of the polymer, respectively; $I_{rxn}(M)$ and $I_{ref}(M)$ are the peak intensities of the reaction and reference peak of the monomer.[9]

Raman spectra of the polymerized films were collected using an optical microscope (DMLP, Leica) connected to a modular research Raman spectrograph (HoloLab 5000R, Kaiser Optical Systems, Inc.) via a 100-μm collection fiber. A single-mode excitation fiber carried an incident beam of a 785-nm near-infrared laser to the sample through a 10x objective with a numerical aperture of 0.25 and a working distance of 5.8 mm. Laser power at the sample was ~10 mW. Spectra were collected with an exposure time of 15 seconds and 3 accumulations. Fifteen monomer spectra were collected and averaged to provide accurate values for $I_{rxn}(M)$ and $I_{ref}(M)$ to use in Eqn 2. Three spectra were collected from different areas of each polymer film and averaged to report conversion.

Dynamic Mechanical Analysis

A dynamic mechanical analyzer (DMA, Q800 TA Instruments) equipped with a film tension clamp was used to find the glass transition temperature (T_g) of the same polymer films used to determine conversion. A mono-frequency strain, temperature ramp sequence was used to collect tan δ values as a function of temperature. Temperature was increased at a rate of 3°C/min over a broad temperature range at a constant oscillating frequency of 1 Hz and a sinusoidal strain of 0.05%. The polymer T_g was taken as the maximum of the tan δ peak.

Results and Discussion:

This study investigated the impact of chemical structure on the magnitude of the dose rate effect. Dose rate effects were monitored by acrylate conversion and the polymer T_g, measured by Raman spectroscopy and DMA, respectively. Using the results of this study, a relationship to predict the dose rate effect for a given formulation was developed for industrial scale-up.

Influence of Dose on Dose Rate Effects

The conversion of the polymer films was measured after exposure to EB radiation. Both dose and line speed were systematically varied to determine the effect of dose on dose rate effects. As expected, due to the increased number of electrons, conversion increases with increasing EB dose for all five monomer/oligomer formulations. A representative set of these data is shown in Table 1.

Table 1. Acrylate conversion (%) for three monomer/oligomer formulations at three different doses and line speeds. Conversion was measured using Raman spectroscopy and calculated using Eqn 2. Conversion increases with increasing dose (at a constant line speed), but decreases at increasing line speed (at a constant dose).

	20 ft/min			100 ft/min			200 ft/min		
	15 kGy	**30 kGy**	**60 kGy**	**15 kGy**	**30 kGy**	**60 kGy**	**15 kGy**	**30 kGy**	**60 kGy**
PA	74	94	98	45	78	90	41	52	76
PEA	96	98	99	62	87	97	55	87	89
HPOPA	96	98	99	96	97	98	93	96	97

Additionally, conversion decreases with increasing the line speed at a given dose. PEA polymerized at 15 kGy, for example, achieved 96% conversion at 20 ft/min but only reached 55% conversion at 200 ft/min. To better evaluate this dose rate effect (DRE) and its trends, a conversion DRE was defined as the change in conversion, at a single dose, as the line speed is increased from 20 ft/min to 200 ft/min, or

$$Conv.DRE(dose) = \left|Conversion_{20ft/min} - Conversion_{200\,ft/min}\right| \quad (3)$$

The conversion DRE for three representative formulations at each of the three doses is shown in Figure 3.

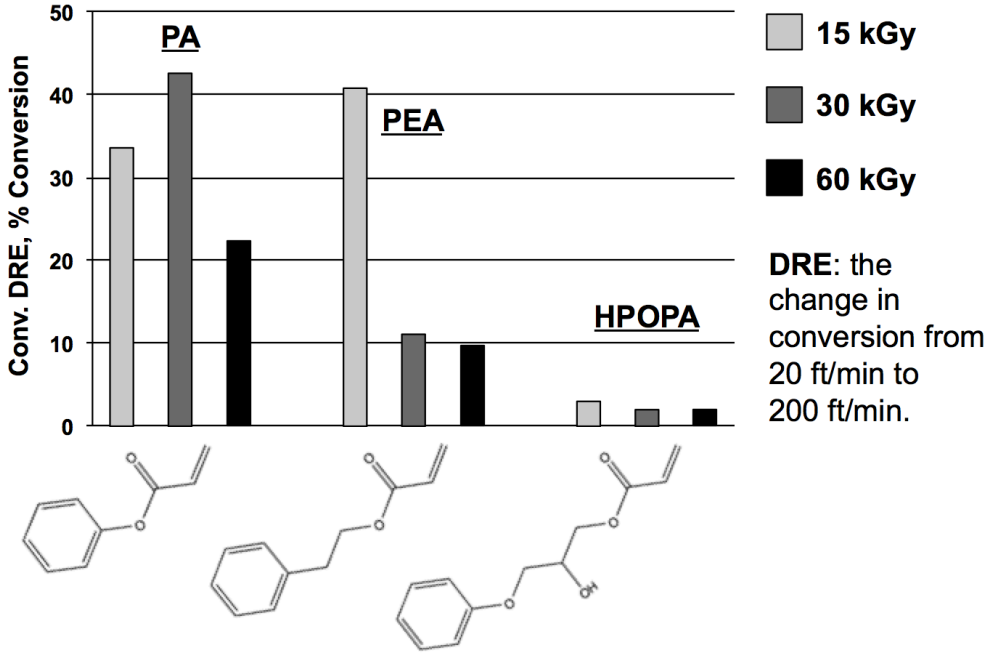

Figure 3. The conversion DREs, at three different doses, for three monomer/oligomer formulations. In general, the DRE magnitude decreases with increasing dose and with increasing monomer size.

With the exception of PA at 15 kGy, the magnitude of the conversion DRE decreases as dose increases for all five monomers. Large decreases in the DRE are observed for PA and PEA (up to 30%) across increasing dose. In contrast, HPOPA shows a very small (< 4%) change in conversion DRE at all three dose levels. The changes in monomer structure may provide an explanation for this trend and will be considered in the following section.

The trends observed with polymer T_g were very similar to those of conversion: as the dose was increased, a corresponding increase was seen in the T_g (Tab 2). The T_g also decreased with increasing line speeds (at a constant dose).

Table 2. Glass transition temperature (T_g, °C) of the EB-cured films for three monomer/oligomer formulations at three different doses and line speeds. T_g was measured using DMA. T_g increases with increasing dose (at a constant line speed), but decreases with increasing line speed (at a constant dose).

	20 ft/min			100 ft/min			200 ft/min		
	15 kGy	**30 kGy**	**60 kGy**	**15 kGy**	**30 kGy**	**60 kGy**	**15 kGy**	**30 kGy**	**60 kGy**
PA	26	49	57	3	31	50	-21	6	19
PEA	17	21	24	-8	10	24	-17	9	18
HPOPA	28	29	30	26	30	30	24	27	28

Parallel to the conversion DRE equation (Eqn 3) and definition, a T_g DRE equation was established to investigate T_g DREs (Eqn 4).

$$T_g\ DRE(dose) = \left|T_{g,20ft/min} - T_{g,200\ ft/min}\right| \quad (4)$$

For each formulation, the magnitude of the T_g DRE decreases as dose is increased from 15 to 60 kGy (a representative set of these data is shown in Figure 4).

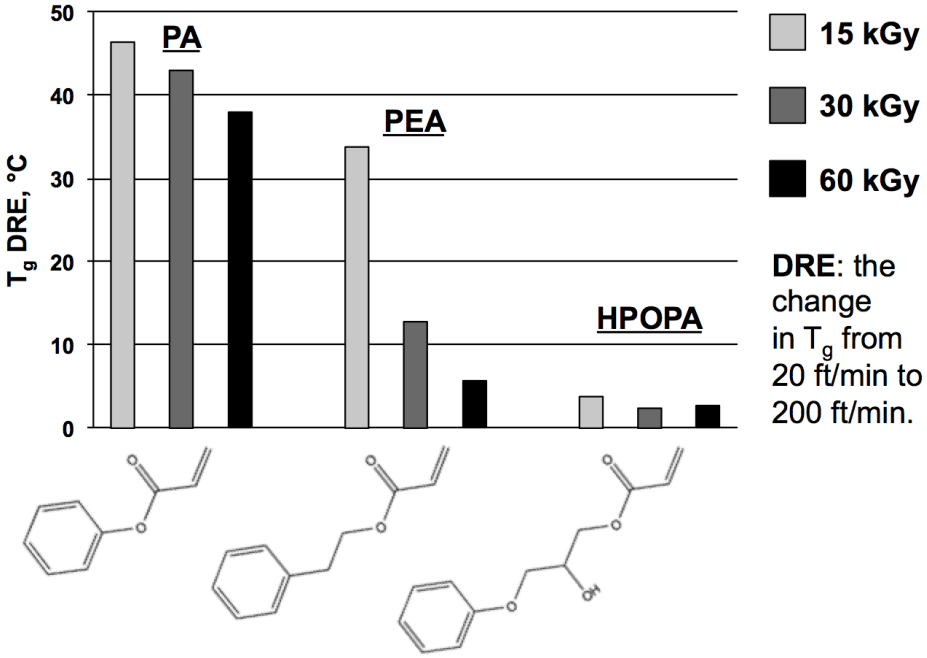

Figure 4. The T_g DREs, at three different doses, for three monomer/oligomer formulations. In general, the DRE magnitude decreases with increasing dose and with increasing monomer size.

However, this decrease in DRE is not necessarily linear. The PEA formulation, for example, experiences a relatively large change (~20°C) in its T_g DRE from 15 to 30 kGy but a relatively smaller DRE shift (~5°C) from 30 to 60 kGy. BA and POEA experience similar trends in T_g DRE as dose is increased. This noted difference suggests that a minimum amount of energy, unique to each monomer chemistry, is required to form the majority of the polymer network. Once this majority network is reached, the T_g is more stable and changes less with increasing dose.

This theory that extent of polymer network formation influences the DRE as dose is increased is corroborated by the DRE conversion trends (Fig 3) and the conversion values (Tab 1). Since the majority of films achieved high conversions (typically ≥ 90%) at 20 ft/min (Tab 1), regardless of dose, Equation 4 shows a decrease in DRE must be due to an increase in polymer conversion at 200 ft/min. Therefore, small conversion DREs indicate a more fully formed polymer network. Only PA does not follow the noted trend; even at 20 ft/min, with a dose of 15 kGy, PA only reached 74% conversion.

This connection between conversion and T_g is well known: the T_g will increase with increasing polymer molecular weight, which in turn increases with conversion, until it reaches a threshold

molecular weight where a maximum T_g is achieved.[10] Furthermore, monomer is known to plasticize the polymer film. At lower conversions, more monomer remains and suppresses the T_g.

Influence of Monomer Structure on Dose Rate Effects

As monomer size decreases across the series, the magnitudes of both the conversion and T_g DREs increase significantly (Figs 3 and 4). The formulation containing HPOPA, the largest molecule in the five-monomer series, shows the lowest DREs in the series in both T_g (4°C) and conversion (3%) at a constant dose of 15 kGy. At the same dose, the smallest molecules (PA and BA) have the largest DREs (51% and 47°C, respectively). This trend may not actually be reflective of the size of the monomer molecule, but rather that the smaller molecules have fewer abstractable hydrogens, which limits chain transfer.

The main process resulting from EB irradiation is the generation of free radicals from ionization (Scheme 1).

Ionization:	$M \xrightarrow{e^-} R^*$
Initiation:	$R^* + M \rightarrow M^*$
Propagation:	$M_n^* + M \rightarrow M_{n+1}^*$
Chain Transfer:	$M_n^* + MH \rightarrow M_nH + M^*$
Termination:	$M_n^* + M_m^* \rightarrow M_{n+m}$

Scheme 1. The EB polymerization reaction mechanism.

In EB polymerization, these radicals are used to initiate the reaction, propagate the growing polymer chain, and eventually terminate the reaction. In the presence of abstractable hydrogens, chain transfer can also occur due to the low bond dissociation energy of C-H and O-H bonds. Each of these kinetic steps is dependent on the concentration of free radicals in the system.

Increasing the dose rate (*dD/dt*) increases the concentration of accelerated electrons at any given moment during an EB reaction, since the same amount of energy must be delivered over a shorter time period; in turn, the concentration of radicals ($[M^*]$) is also increased. Increasing the concentration of radicals increases the rate of propagation, R_p,

$$R_p = k_p[M][M^*] \tag{5}$$

where k_p is the propagation rate constant and [M] is the concentration of monomer. The rate of termination, R_t, also increases when the radical concentration is increased,

$$R_t = k_t[M^*]^2 \tag{6}$$

where k_t is the termination rate constant. However, the relationship between radical concentration and rate is first order for the rate of propagation and second order for the rate of termination. Thus, increasing the radical concentration causes a larger increase in the termination rate than in the propagation rate, leading to shorter polymer chains and lower conversions. Kinetically, dose rate effects are expected. Yet, as observed in Figures 3 and 4, the magnitude of DREs can vary widely. Equations 5

and 6 are not expected to account for this variability in DRE, since the rate constants (k_p and k_t) should not change significantly for similar acrylate monomers.

A notable difference between the five monomers investigated, however, is the quantity of abstractable hydrogens (Fig 1). Setting aside the hydrogen atoms the monomers have in common (on the phenyl ring and acrylate moiety), PA, for example, does not contain any additional hydrogen atoms; in contrast, HPOPA has five potentially abstractable hydrogen atoms, including a tertiary hydrogen atom alpha to an oxygen atom that should be easily abstracted due to the low bond energy (4.4 eV).[11] Increasing the concentration of abstractable hydrogens ([*MH*]) increases the rate of chain transfer (R_{ct}):

$$R_{ct} = k_{ct}[M^*][MH] \tag{7}$$

where k_{ct} is the chain transfer rate constant. Chain transfer provides a route to conversion by effectively untethering the propagating radical from an entangled polymer chain, increasing the radical's ability to diffuse through the system and reach unreacted monomer molecules. Therefore, if the monomer structure is conducive to a higher rate of chain transfer, the combined propagation and chain transfer mechanisms can compete more effectively with termination, leading to higher conversion. At low dose rates, where high conversions (>90%) are achievable, the aid of the chain transfer mechanism may go unnoticed; however, when the dose rate is increased, and with it R_t is increased exponentially faster than R_p, it is possible that promoting chain transfer restores the balance between termination and conversion, lessening or eliminating dose rate effects. This explanation is consistent with the relative order of DREs for the monomers in this study.

Predicting Dose-Rate-Effect Magnitude

The results discussed above demonstrate that the T_g of a polymer produced via EB initiation can be increased by increasing the dose or by decreasing the dose rate (Tab 2 and Fig 4). These results were used to develop a predictive correlation between the magnitude of the T_g DRE and the T_g shift caused by a formulation's response to different doses. The latter is defined as the T_g dose effect (DE, Eqn 8).

$$T_g\ DE(line\ speed) = \left|T_{g,60kGy} - T_{g,15kGy}\right| \tag{8}$$

Specifically, in this five-monomer series, the change in polymer properties caused by a 4-fold increase in dose (15 to 60 kGy) was found to be equivalent to the property change caused by a 10-fold increase in line speed (20 to 200 ft/min).

To demonstrate this relationship between dose and line speed, Figure 5 compares the change in T_g caused by the increase in dose (15 to 60 kGy) at 20 ft/min [T_g DE (20 ft/min)] to the change in T_g caused by the increase in line speed (20 to 200 ft/min) at 60 kGy [T_g DRE (60 kGy)].

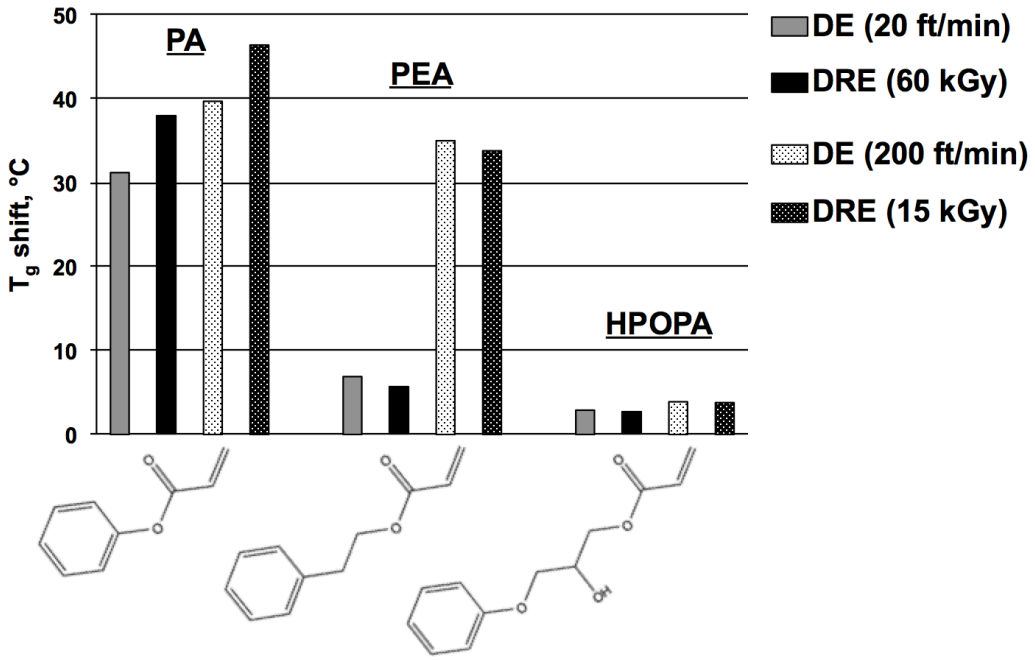

Figure 5. Using T_g-shift comparisons, a demonstration of the relationship between increasing dose 4-fold and line speed 10-fold. DE (20 ft/min) is the magnitude of the T_g shift from 15 kGy to 60 kGy at a constant line speed of 20 ft/min. DRE (60 kGy) is the magnitude of the T_g shift from 20 ft/min to 200 ft/min at a constant dose of 60 kGy. To be perfectly predictive, the bar values in gray should be equal to those in black, and light-textured bar values should equal dark-textured bar values.

The same relationship is also shown for an increase in dose at 200 ft/min [T_g DE (200 ft/min)] and an increase in line speed at 15 kGy [T_g DRE (15 kGy)] (Fig 5, textured bars). To be accurately predictive, the T_g shift of the corresponding DE and DRE should be equal. The DE magnitude is within 2°C of that of the DRE for the PEA, POEA, and HPOPA formulations. The largest difference between T_g shifts is approximately 7°C for the PA and BA formulations. This error in prediction is expected to decrease with replication of the results. Even with current level of error, the T_g of the final BA film was predicted to within 4°C of the actual experimental value using this DE-DRE relationship.

The correlation between DE and DRE for EB-polymer properties (in this case, T_g), is significant because it allows for the prediction of DREs by simply changing the dose. DREs often may only be observed at high processing speeds, which are difficult to achieve in a lab or pilot-line setting; however, dose is easily adjusted in either situation.

Conclusions:

This study has demonstrated clear DRE trends, as measured by shifts in the conversion and T_g of EB-polymerized films. It was established DREs are dependent on dose: as dose was increased, the magnitude of the dose rate effect decreased. The size of the DRE was also shown to be highly dependent on the chemical structure of the monomer: the magnitude of the DRE increased across the five-monomer series, having the largest effects on the smallest molecule, PA. This influence of monomer structure on the DRE trend was consistent with the expected differences in the rate of chain transfer contributed by the relative number of abstractable hydrogens. Furthermore, this work has shown that predictions can be made about the magnitude of a formulation's DRE by comparing its

response to different doses (DE). These DRE predictions are useful for industrial scale-up, as well as the establishment of a fundamental kinetic foundation that EB polymerization currently lacks. Future studies will determine the efficacy of this predictive relationship for a broad range of monomers and will explore how reaction kinetics support the 4-to-10 ratio of dose to line speed.

Confirming DREs in both conversion and T_g and establishing similar DRE trends in both polymer properties are integral steps for future investigations. This study examined DREs on monomer/oligomer formulations because the inclusion of oligomers was necessary to achieve films with enough structural integrity for DMA measurements. Although the oligomer chemistry remained constant, it would be preferable to study DREs on pure monomers. Similarly, the presence of a phenyl ring in the monomer structure was needed for Raman measurements, yet few acrylate monomers contain a phenyl ring. By comparing conversion and T_g results in a formulation series that could withstand both Raman spectroscopy and DMA, series can now be developed that can only be explored using one method or the other with reasonable certainty that the presence of conversion DREs will indicate T_g DREs and vice versa. Structural integrity is not needed for Raman, thus the effect of oligomers can be studied by comparing current conversion results with those of pure monomer formulations. A phenyl monomer is not needed for DMA experiments, thus widening the field of acrylates that can be investigated.

Taken collectively, the results of this study have established a rudimentary structure/processing conditions/properties relationship. Albeit preliminary and only confirmed for this 5-monomer acrylate series, understanding how the chemical structure of the starting materials and the processing conditions they undergo collectively influence the final properties of the polymer produced is vital to understanding the fundamental aspects of EB polymerization and furthering the development of EB technology. As future studies strengthen this structure/processing conditions/properties relationship, this knowledge can be used to expand EB technology to create high-performance EB materials at high production speeds.

Acknowledgements:

This material is based upon work supported by the National Science Foundation under Grant No. 1264622 and The University of Iowa Mathematical & Physical Sciences Funding Program. The authors would also like to acknowledge Kathryn Classon and Shiqin He for their contributions with sample preparation.

References:

(1) Cohen, G. *RadTech Report* **2012**, No. 2, 44–48.
(2) Datta, S. K.; Chaki, T. K.; Bhowmick, A. K. **2000**, 1–30.
(3) *Radiation Curing of Polymeric Materials*; Hoyle, C. E., Kinstle, J. F., Eds.; American Chemical Society, 1990.
(4) Drobny, J. G. *Ionizing Radiation and Polymers*; Elsevier Inc., 2013.
(5) Richter, K. B. **2007**, 1–246.
(6) Weiss, D. E.; Dunn, D.; Richter, K. B.; Adler, R. **2005**, 1–11.
(7) Burth, D.; Lechner, V.; Krebs, F. *RadTech Report* **2010**, 34–41.
(8) Schissel, S. M.; Lapin, S. C.; Jessop, J. L. P. *RadTech Report* **2014**, No. 4, 46–50.
(9) Cai, Y.; Jessop, J. L. P. *Polymer* **2006**, *47* (19), 6560–6566.
(10) Odian, G. *Principles of Polymerization*, 4 ed.; John Wiley and Sons, Inc., 2004.

(11) Darwent, B. D. *Bond Dissociation Energies in Simple Molecules*; U.S. Government Printing Office: Washington, D.C., 1970; pp 1–58.